ACS Chemical Neuroscience

Letter

pubs.acs.org/chemneuro

An Early Folding Contact between Phe19 and Leu34 is Critical for Amyloid-β Oligomer Toxicity

Anand K. Das,[†,§] Anoop Rawat,[†,§] Debanjan Bhowmik,[†] Rucha Pandit,[†] Daniel Huster,[‡] and Sudipta Maiti*[,†]

[†]Department of Chemical Sciences, Tata Institute of Fundamental Research, Homi Bhabha Road, Colaba, Mumbai 400005, India

[‡]Institute of Medical Physics and Biophysics, University of Leipzig, Härtelstr. 16-18, D-04107 Leipzig, Germany

ABSTRACT: Small hydrophobic oligomers of aggregation-prone proteins are thought to be generically toxic. Here we examine this view by perturbing an early folding contact between Phe19 and Leu34 formed during the aggregation of Alzheimer's amyloid-β ($A\beta_{40}$) peptide. We find that even conservative single mutations altering this interaction can abolish $A\beta_{40}$ toxicity. Significantly, the mutants are not distinguishable either by the oligomers size or by the end-state fibrillar structure from the wild type $A\beta_{40}$. We trace the change in their toxicity to a drastic lowering of membrane affinity. Therefore, nonlocal folding contacts play a key role in steering the oligomeric intermediates through specific conformations with very different properties and toxicity levels. Our results suggest that engineering the folding energy landscape may provide an alternative route to Alzheimer therapeutics.

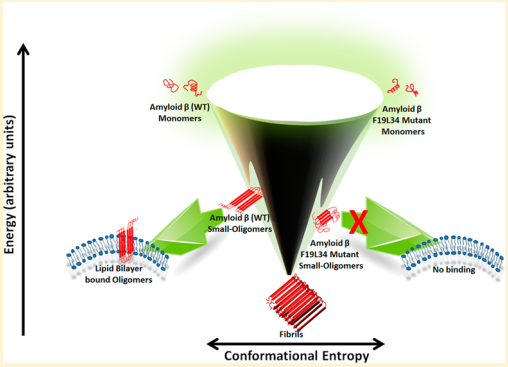

KEYWORDS: *Protein aggregation, neurodegeneration, folding landscape, small oligomers, membrane affinity, Alzheimer therapeutics*

The origins of many age-related incurable disorders have been linked to the aggregation of amyloid proteins.[1] Specifically, small oligomeric intermediates in the aggregation pathway have been identified as the major toxic species.[2,3] Some structural models of mature fibrils,[4−10] large oligomers,[11,12] and recently also of the small oligomers[13] have been derived from solid-state NMR experiments. However, these structural data have not shed much light on what makes these oligomers toxic or the fibrils less toxic. It has been suggested that the small size and hydrophobic surfaces of protein oligomers ensure that these particles have high affinity for biological membranes, and therefore they are generically toxic.[14] This view is supported by the toxicity observed for the oligomers of many disease-unrelated proteins, whose oligomers can be produced in vitro.[15−17] However, this generalization ignores the possibility that toxicity may also strongly depend on specific conformations,[18] which are dictated by nonlocal folding contacts. If so, even conservative (e.g., hydrophobic to hydrophobic) mutations may alter the aggregation pathway, making the oligomers nontoxic, but leading to the same final fibrillar state. If true, it would suggest an alternative therapeutic strategy which does not attempt to alter aggregation per se, but engineers the folding/aggregation free-energy landscape such that the population passes through nontoxic routes.

Until now, only nonconservative single mutations of amyloid-β ($A\beta$) have been observed to exert a protective effect in AD. For example, A2T has been found to be protective,[19−21] while another mutation, A2V, has dominant negative effect on $A\beta$ amyloidogenesis.[21−23] This indicates the importance of the second amino acid in the unstructured N-terminal domain of $A\beta$ in polymerization and toxicity. Here we focus on the well-preserved F19-L34 contact in the $A\beta$ aggregates. This is a nonlocal contact observed in almost all $A\beta$ aggregates investigated at the atomic level.[6,12,13,24−26] This contact forms early, and is observed in the protofibrils[26] and even in the small oligomeric intermediates (n-mers with $n < 10$) which form during the initial phase of in vitro aggregation.[13] These oligomers have significant β-sheet content,[11,27−29] while the monomers are mostly unfolded with some α-helical content.[30−32] They also develop an order of magnitude higher membrane affinity compared to the monomers,[33−35] suggesting a connection between folding and the evolution of toxicity for these extracellular peptides.

We investigate six single mutations which replace F19 and two double mutations which replace both F19 and L34 by hydrophobic, neutral, polar, and charged residues. These physiologically nonrelevant mutations were designed to perturb the $A\beta$ structure formation process by local physical forces. To probe the effect of maximum and minimum conformational flexibility, phenylalanine residue at position 19 was replaced by glycine (F19G) and proline (F19P), respectively. Next, alterations were done with negatively charged glutamate (F19E) and with positively charged lysine (F19K) residues which would render these positions hydrophilic (from highly hydrophobic). Also, F19 was replaced by tyrosine (F19Y) and tryptophan (F19W), to investigate the effects of altered hydrogen bonding and/or hydrophobic contacts without changing the overall hydrophobic nature of the interaction.

Published: May 7, 2015

DOI: 10.1021/acschemneuro.5b00074
ACS Chem. Neurosci. 2015, 6, 1290−1295

The double mutation F19K L34E was designed to replace the hydrophobic contact with a salt bridge, while the F19K L34K mutation was designed to strongly perturb this contact by electrostatic repulsion.

Solid-state NMR studies performed earlier have already shown that for all but one of these mutations, namely, F19K L34E, the mature fibrillar aggregates have very similar structures.[36] Therefore, these perturbations can at best have an effect on the pathway and the kinetics of aggregation, but not on the end product. However, if toxicity is a generic property of small oligomers, then such pathway engineering would be expected to have minimal effects on the toxicity (provided the mutants form oligomers of size and stability similar to that of the wild type peptide). Here we measure the toxicity of these oligomers on rat primary cortical neuronal cultures. We also measure the oligomer size and the membrane affinity of these oligomers, and correlate the observed toxicity changes with these two parameters.

We have earlier established the protocol to prepare oligomer-rich solutions of Aβ.[37] Briefly, purified peptide powders were initially dissolved in water at pH 11 (pH adjusted by NaOH) to prepare clear stock solutions and then diluted to required concentrations in physiological buffer solutions at pH 7.4. To probe the cytotoxicity of WT Aβ_{40} and the eight mutant species on rat primary cortical neurons, we prepare 100 μM of the peptide solution in cell culture medium and incubate them with primary neurons for 60 h. We checked the stability of the WT Aβ_{40} and the mutant peptides under these conditions using mass spectrometry, and found them to be stable over this duration (data not shown). We use relatively high concentrations of the peptides since cell death is difficult to observe in the laboratory time scale at physiological concentrations. At 100 μM Aβ concentration, fibrillar and protofibrillar species will begin to form within hours. However, our earlier studies have shown that even as larger particles form due to aggregation, small oligomers (presumably the major toxic species) continue to exist in the solution for a long time.[38,39] Same situation is likely to prevail in these experiments. Cell viability was assessed using 0.01 mg/mL of propidium iodide (PI) and 0.01 mg/mL of Hoechst 33342 dyes. The ratio of the number of cells stained with PI to the cells stained with Hoechst 33342 provides a measurement for the percentage of dead cells. The data is expressed as percent cell viability relative to vehicle treated control cells. The viability of control cells was normalized to be 100% (actual viability of control cells was 70 ± 4%). As shown in Figure 1, the relative cell viability of WT Aβ_{40} was 40 ± 6%. This is very different from the conformationally flexible F19G mutant (95 ± 4%) and its more rigid and structurally confined counterpart, the F19P mutant (89 ± 4%).[36] Alterations with charged residues F19E (98 ± 5%) and F19K (94 ± 4%) too had minimal effect on cell viability. The F19Y and F19W mutants showed viability of 91 ± 5% and 98 ± 6%, respectively, indicating that the mutants which retain much of the hydrophobicity but possibly with altered hydrogen bonding and hydrophobic contacts are also benign. Replacement of the hydrophobic contact F19-L34 by a salt bridge, F19K L34E, also had no detrimental effects on cell viability (94 ± 4%). When the contact was replaced with two similarly charged residues, F19K L34K, the cell viability turned out to be 96 ± 5%. While the difference between the control and the mutants are not statistically significant at $p < 0.05$ level, the WT peptide was significantly toxic ($p < 0.001$). Thus, any alteration to the nonlocal contact, F19-L34, drastically lowers the toxicity of the peptide.

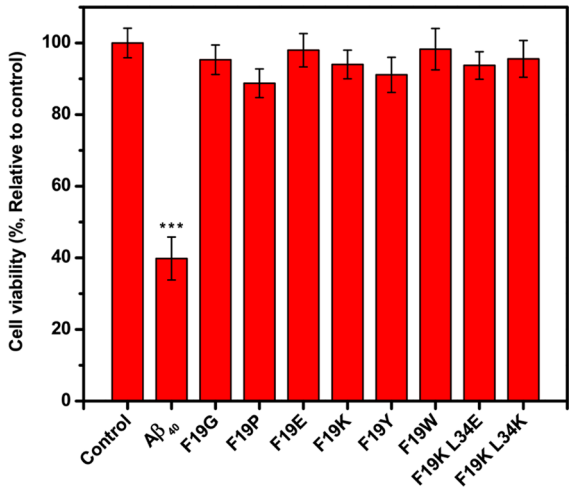

Figure 1. Cell viability assay. Primary cortical neuronal cultures were treated with 100 μM of Aβ_{40} and the different mutants. Cell viability was assessed after 60 h of incubation using Hoechst/PI staining. Values represent mean ± SEM. ***Indicates that the difference is statistically significant ($p < 0.001$).

One possibility is that these mutants do not even form oligomers of size similar to that of the WT Aβ_{40}. This can be easily tested with the help of fluorescence correlation spectroscopy (FCS).

We prepared 100 nM solutions of rhodamine-B labeled WT Aβ_{40} and mutant Aβ_{40} in phosphate-buffered saline (PBS) at pH 7.4 and performed FCS measurements on these specimens with an instrument constructed in-house.[40] FCS and its several variants are effective tools for following protein aggregation.[41−44] FCS data were fitted with a discrete one/two components diffusion model using the Origin 7 software (OriginLab Corporation). The data were converted into hydrodynamic radii (R_H) using rhodamine-B (R_H = 0.57 nm[45]) as a calibrant. For clarity, the representative autocorrelation curves obtained from WT Aβ_{40} and only three of the eight mutants (F19G, F19K, and F19W) are shown in Figure 2A. These data were fitted with a single diffusion component. The bar graph (Figure 2B) shows the size (hydrodynamic radii) for WT Aβ_{40} and all eight mutants. We find that all the mutants formed oligomers with reasonably similar hydrodynamic radii compared to WT Aβ_{40}. Thus, perturbation of the nonlocal hydrophobic contact, F19-L34, seems to have no major effect on the size of the oligomers formed. Hence the roots of toxicity (or the lack of it) are likely to lie in the different conformations adopted by the peptide in these similar-sized oligomers.

We then ask if there is a quantifiable physical property which can explain the low toxicity of these mutants. We have shown earlier that the wildtype (WT) oligomers have at least an order of magnitude higher membrane affinity than the nontoxic monomers.[33] Since Aβ is an extracellular peptide, membrane binding is an expected first step of toxicity, and we hypothesized that this aspect may be different for the mutants. However, it is difficult to quantitatively measure the affinity of Aβ to cell membranes, because of the intrinsic background present in the membranes, and the variability in the membrane conditions. A vesicle binding assay can provide a quantitative measure for the membrane-affinity of different Aβ species.[35]

DOI: 10.1021/acschemneuro.5b00074
ACS Chem. Neurosci. 2015, 6, 1290−1295

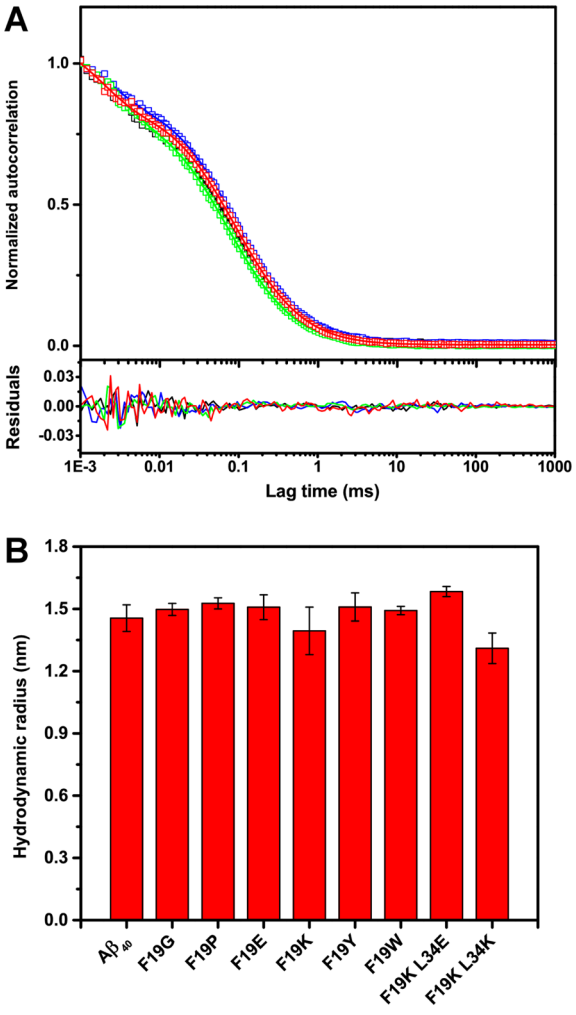

Figure 2. Oligomer size in solution. (A) Representative normalized autocorrelation of select peptide oligomers in solution. Open symbols, data; solid lines, fit (upper panel), residuals (lower panel). Black, Aβ_{40}; blue, F19G; green, F19K; red, F19W. (B) Oligomer size (R_H) of Aβ_{40} and mutants in buffer. Values represent mean ± SD.

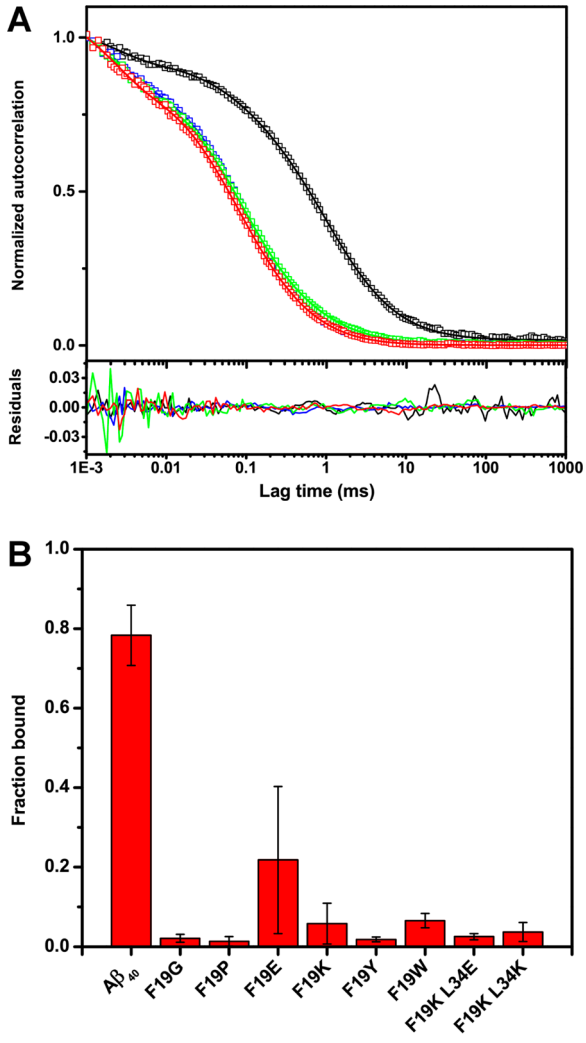

Figure 3. Vesicle binding by oligomers. (A) Representative normalized autocorrelation of select peptides in the presence of vesicles. Open symbols, data; solid lines, fit (upper panel), residuals (lower panel). Black, Aβ_{40}; blue, F19G; green, F19K; red, F19W. (B) Binding of Aβ_{40} and mutants oligomers to PPC 111 vesicles. Values represent mean ± SD.

We have therefore used this method here for comparing the relative binding affinities of the peptides.

We investigated the vesicle binding affinity of each of the above mutant species. To this end, we prepared lipid membranes composed of POPC (1-palmitoyl-2-oleoyl-*sn*-glycero-3-phosphocholine), POPG (1-palmitoyl-2-oleoyl-*sn*-glycero-3 phosphoglycerol), and cholesterol in molar ratio 1:1:1 (PPC 111). Unilamellar PPC 111 vesicles were prepared by sonication in physiological buffer. The hydrodynamic radii (R_H) of the vesicle solutions were measured by FCS using the lipid binding dye, Nile red, which yielded an average R_H of 18−50 nm (in different sets of experiments). The freshly prepared oligomeric solutions of rhodamine-B labeled WT Aβ_{40} and mutant peptides were separately incubated for 30 min each with the PPC 111 vesicles. The vesicle solutions were then examined with FCS. The data from the vesicle containing solution were fitted to a model incorporating two diffusion components. The appearance of a slow component consistent with vesicle size would imply that oligomers had attached to the vesicles. For clarity, the autocorrelation curves in the presence of vesicles are shown only for the WT and the three mutant species F19G, F19K, and F19W (Figure 3A). The FCS autocorrelation curves plotted on a semilogarithmic scale give a visual indication of fast and slow diffusing species. The autocorrelation of a fast diffusing species would decay faster than that of a slow diffusing one. As is evident from Figure 3A, in the presence of lipid vesicles, diffusion of WT Aβ_{40} is slower (autocorrelation curve shifts toward the right) compared to the mutants. This indicates that WT Aβ_{40} oligomers have attached to lipid vesicles which due to their large size would diffuse comparatively slowly. Oligomers from mutant peptides on the other hand do not bind lipid vesicles and hence exhibit faster decaying autocorrelation curves. A quantitative estimation of oligomer attachment to lipid vesicles can be carried out by fitting the FCS autocorrelation curves with a two-component model, where the fast diffusing component represents free oligomers in solution, and the slow diffusing component represents vesicle-bound oligomers. The ratio of the amplitude of slow diffusing component to the sum of the amplitudes of the two components yields the fraction of peptide bound to lipid vesicles. This quantity is presented in Figure 3B.We note that the vesicles do have a distribution of sizes. However, using

DOI: 10.1021/acschemneuro.5b00074
ACS Chem. Neurosci. 2015, 6, 1290−1295

a quasi-continuum fitting routine (MEMFCS[46]), we separately verify that the size distribution is narrow, and a two component fit for the data is valid (analysis is not shown). In case of WT Aβ_{40}, the smaller component (corresponding to the free oligomeric fraction) was 1.5 ± 0.6 nm (amplitude 22%) while the larger vesicle-bound component was 17 ± 1.6 nm (amplitude 78%). Figure 3B shows the vesicle-bound fraction for all the mutants. Interestingly, while the WT Aβ_{40} showed considerable binding (78 ± 8%), all the mutants exhibited much lower binding compared to the WT. F19G, F19P, F19Y, F19K L34E, and F19K L34K mutants have very similar binding affinity to the vesicles: 2 ± 1, 1.4 ± 1.2, 2 ± 0.6, 3 ± 0.8, and 4 ± 2%, respectively. The other three mutants show somewhat higher binding affinity, but the values are still substantially lower than the WT. F19E shows 22 ± 19%, while F19K and F19W show 6 ± 5% and 7 ± 2% binding, respectively. The nonlocal contact between residues 19 and 34 is therefore important for defining the specific conformation which makes them competent to bind to vesicle membranes. This is consistent with our toxicity measurements, since the inability of an extracellular peptide to efficiently bind to the cell membrane will also imply a lowering of its toxicity.

CONCLUSIONS

Our results show that specific structural details, such as a single nonlocal contact, can completely change the membrane-affinity and toxicity of the transient oligomers, at least for Aβ_{40}. As the unstructured monomers of Aβ aggregate to form the early oligomeric intermediates,[47] it also folds into a hairpin-like shape.[18] Early folding contacts can be major determinants of the structures adopted by the evolving aggregation intermediates, though they may have a lesser role in defining the ultimate folded structure. Our results indeed show that a perturbation of the F19-L34 contact can drastically reduce the membrane affinity of the Aβ oligomers. Interestingly, it appears that the contact is not merely of a nonspecific hydrophobic nature, since conservative substitutions by other hydrophobic residues still lower the membrane affinity. This suggests that a steric match between these two residues is important in driving the evolution of Aβ oligomers. Such "steric zippering" has indeed been suggested for the evolution of Aβ and other aggregates.[48]

A major implication of our results is that the folding free-energy landscape can be modulated such that the end-state remains similar, but the intermediates are completely different. Such "landscape engineering" would have a lower thermodynamic cost compared to the disaggregation of fibrils. While the mature fibrils, which represent the final structure in the Aβ folding pathway, are not perturbed significantly,[36] the altered energy landscape has a profound impact on the intermediates and their immediate toxicity. This might suggest a new pharmaceutical strategy for tackling Alzheimer's disease: develop agents which raise the free-energy cost of forming the F19-L34 contact. The candidate drug may be a small peptide, an antibody (or a small antibody mimetic), or even an organic molecule which has some specific interaction with this region of the Aβ peptide. Since such an agent would have to work only with the intermediates, it may even be able to work in a substoichiometric catalytic manner.

METHODS

Peptide Synthesis. Wildtype (WT) Aβ_{40} and mutated Aβ_{40} peptides were synthesized using standard Fmoc solid phase synthesis strategy as described earlier.[36]

Primary Cortical Neuronal Cultures. Pregnant female Wistar rats were obtained from the TIFR Animal Facility. All animal handling procedures were approved by the Animal Ethics Committee of TIFR. Briefly, neurons were isolated from cortex of 17day old embryos which were subdissected under sterile conditions in Hank's balanced salt solution (HBSS) containing HEPES, 50 units/mL penicillin, and 50 μg/mL streptomycin. This was followed by trypsin digestion (0.25% solution) for 15−20 min at room temperature, with subsequent trituration and plating on poly-L-lysine coated 96-well plates. The cell culture media comprised neurobasal A supplemented with 2% b-27 supplement, 0.5% penicillin-streptomycin, and 0.25% L-glutamine. The culture media was changed every 48 h.

Toxicity Assay. The cell toxicity assay was performed with 100 μM of the peptides incubated with 3 day old rat primary cortical neuronal cultures grown in 96-well plates. The extent of cell death was assessed after 60 h using Hoechst/PI staining. In brief, the cells were treated with 0.01 mg/mL propidium iodide (PI, DNA intercalating dye that labels only the dead cells) and 0.01 mg/mL Hoechst 33342 (DNA intercalating dye that labels both live and dead cells) in Thomson's buffer (TB, consisting of 20 mM sodium HEPES, 146 mM NaCl, 5.4 mM KCl, 1.8 mM $CaCl_2$, 0.8 mM $MgSO_4$, 0.4 mM KH_2PO_4, 0.3 mM Na_2HPO_4, and 5 mM dextrose; pH adjusted to 7.4) for 10 min followed by washing with TB. The cells were imaged for Hoechst 33342 and PI fluorescence in a confocal microscope setup (LSM-710, Zeiss, Germany) using a 20× objective. Two photon excitation of Hoechst 33342 was performed using 690 nm pulsed light from a mode-locked Ti-sapphire laser (MaiTai, Spectra Physics, CA). The fluorescence was separated from the excitation using a 690 nm dichroic mirror and detected using a photomultiplier tube (385−535 nm). PI was excited using a 543 nm laser (He−Ne, Zeiss); the fluorescence was separated using a dichroic mirror and detected between 565 and 720 nm. Image analysis was performed for several fields (at least 120 for each peptide) in multiple dishes (16 for each peptide) and scored for the total number of cells (Hoechst 33342 fluorescent spots) and the number of dead cells (PI fluorescent spots) using an automated particle counter in ImageJ (open source software, available from the Web site http://rsbweb.nih.gov/ij/). The ratio of cells which were alive (PI negative) to total cells was reported as viability. The cell viability expressed as percentage was normalized with respect to control cell viability where the control cell viability was assumed to be 100% (actual viability in control cells was 70 ± 4%).

Vesicle Preparation. Small unilamellar vesicles (SUVs) composed of POPC (1-palmitoyl-2-oleoyl-*sn*-glycero-3-phosphocholine), POPG (1-palmitoyl-2-oleoyl-*sn*-glycero-3-phosphoglycerol), and cholesterol in a 1:1:1 molar ratio (PPC 111) were prepared by sonication in phosphate buffered-saline (PBS) containing 20 mM Na_2HPO_4, 150 mM NaCl, and 5 mM KCl at pH 7.4 as described earlier.[35]

FCS Measurements. FCS measurements were performed with an instrument constructed in-house.[40] To measure the size of oligomers of rhodamine-B labeled WT Aβ_{40} and mutants, 100 nM solutions of the peptides were taken separately in PBS buffer at pH 7.4 and FCS measurements were made. FCS data were fitted with discrete one/two-component diffusion model using Origin 7 software (OriginLab Corporation). The FCS data was converted into hydrodynamic radii (R_H) using rhodamine B (R_H = 0.57 nm[45]) as a calibrant. The hydrodynamic radius (R_H) and concentration of the vesicle solutions was characterized by performing FCS with the lipid binding dye, Nile red. The hydrodynamic radius of PPC 111 vesicles was determined to be between 18 and 50 nm (in different sets of experiments).

Vesicle Attachment Studies. Oligomeric solutions (100 nM) of rhodamine-B labeled WT Aβ_{40} and mutant peptides were separately incubated for 30 min with small unilamellar vesicles composed of PPC 111. The vesicles were unlabeled. Attachment of the labeled peptides to the vesicles was probed by FCS. Appearance of a slow diffusing component consistent with the vesicle size implied vesicle binding.

DOI: 10.1021/acschemneuro.5b00074
ACS Chem. Neurosci. 2015, 6, 1290−1295

Statistical Analysis. Data are expressed either as mean ± SEM or mean ± SD as indicated. Toxicity experiments were performed with batches of six to eight wells in a 96-well plate for each peptide. Three independent repeats of these measurements were performed. Multiple fields (~10) were recorded from each dish, giving a total of ~100 readings for each peptide for each repeat. p values required for tests of significance were calculated manually. The FCS experiments with oligomers and vesicle binding were repeated three times independently.

AUTHOR INFORMATION

Corresponding Author

*E-mail: maiti@tifr.res.in.

Author Contributions

[§]A.K.D. and A.R. contributed equally to this work.

A.K.D. performed all the biological experiments and helped write the paper, A. R. performed most of the in vitro experiments, D.B. performed the initial in vitro experiments, R.P. helped in the biological experiments and recorded the mass spectra of the peptides, D.H. and S.M. conceptualized the experiments, S.M. oversaw the data analysis and co-wrote the paper.

Funding

S.M. acknowledges support from the Department of Biotechnology, Government of India (Grant No. BT/53/NE/TBP/2010). D.H. would like to acknowledge support from the German Research Foundation (DFG SFB TRR 102, A6).

Notes

The authors declare no competing financial interest.

ABBREVIATIONS

AD, Alzheimer's disease; Aβ, amyloid β; WT, wild type; FCS, fluorescence correlation spectroscopy; MEMFCS, Maximum entropy method based FCS analysis; R_H, hydrodynamic radius; PBS, phosphate buffered saline; TB, Thomson's buffer; PI, propidium iodide; PPC, POPC ((1-palmitoyl-2-oleoyl-*sn*-glycero-3-phosphocholine); POPG, (1-palmitoyl-2-oleoyl-*sn*-glycero-3-phosphoglycerol), and cholesterol

REFERENCES

(1) Chiti, F., and Dobson, C. M. (2006) Protein misfolding, functional amyloid, and human disease. *Annu. Rev. Biochem. 75*, 333−366.

(2) Benilova, I., Karran, E., and De Strooper, B. (2012) The toxic Aβ oligomer and Alzheimer's disease: an emperor in need of clothes. *Nat. Neurosci. 15*, 349−357.

(3) Haass, C., and Selkoe, D. J. (2007) Soluble protein oligomers in neurodegeneration: lessons from the Alzheimer's amyloid β-peptide. *Nat. Rev. Mol. Cell Biol. 8*, 101−112.

(4) Petkova, A. T., Ishii, Y., Balbach, J. J., Antzutkin, O. N., Leapman, R. D., Delaglio, F., and Tycko, R. (2002) A structural model for Alzheimer's β-amyloid fibrils based on experimental constraints from solid state NMR. *Proc. Natl. Acad. Sci. U. S. A. 99*, 16742−16747.

(5) Luhrs, T., Ritter, C., Adrian, M., Riek-Loher, D., Bohrmann, B., Dobeli, H., Schubert, D., and Riek, R. (2005) 3D structure of Alzheimer's amyloid-β(1−42) fibrils. *Proc. Natl. Acad. Sci. U. S. A. 102*, 17342−17347.

(6) Bertini, I., Gonnelli, L., Luchinat, C., Mao, J., and Nesi, A. (2011) A new structural model of Aβ_{40} fibrils. *J. Am. Chem. Soc. 133*, 16013−16022.

(7) Colletier, J.-P., Laganowsky, A., Landau, M., Zhao, M., Soriaga, A. B., Goldschmidt, L., Flot, D., Cascio, D., Sawaya, M. R., and Eisenberg, D. (2011) Molecular basis for amyloid-β polymorphism. *Proc. Natl. Acad. Sci. U. S. A. 108*, 16938−16943.

(8) Lopez del Amo, J. M., Schmidt, M., Fink, U., Dasari, M., Fandrich, M., and Reif, B. (2012) An asymmetric dimer as the basic subunit in Alzheimer's disease amyloid β fibrils. *Angew. Chem., Int. Ed. Engl. 51*, 6136−6139.

(9) Lu, J. X., Qiang, W., Yau, W. M., Schwieters, C. D., Meredith, S. C., and Tycko, R. (2013) Molecular structure of β-amyloid fibrils in Alzheimer's disease brain tissue. *Cell 154*, 1257−1268.

(10) Mithu, V. S., Sarkar, B., Bhowmik, D., Chandrakesan, M., Maiti, S., and Madhu, P. K. (2011) Zn^{++} binding disrupts the Asp^{23}-Lys^{28} salt bridge without altering the hairpin-shaped cross-β structure of Aβ_{42} amyloid aggregates. *Biophys. J. 101*, 2825−2832.

(11) Chimon, S., Shaibat, M. A., Jones, C. R., Calero, D. C., Aizezi, B., and Ishii, Y. (2007) Evidence of fibril-like β-sheet structures in a neurotoxic amyloid intermediate of Alzheimer's β-amyloid. *Nat. Struct. Mol. Biol. 14*, 1157−1164.

(12) Ahmed, M., Davis, J., Aucoin, D., Sato, T., Ahuja, S., Aimoto, S., Elliott, J. I., Van Nostrand, W. E., and Smith, S. O. (2010) Structural conversion of neurotoxic amyloid-β_{1-42} oligomers to fibrils. *Nat. Struct. Mol. Biol. 17*, 561−567.

(13) Sarkar, B., Mithu, V. S., Chandra, B., Mandal, A., Chandrakesan, M., Bhowmik, D., Madhu, P. K., and Maiti, S. (2014) Significant structural differences between transient amyloid-β oligomers and less-toxic fibrils in regions known to harbor familial Alzheimer's mutations. *Angew. Chem., Int. Ed. Engl. 53*, 6888−6892.

(14) Mannini, B., Mulvihill, E., Sgromo, C., Cascella, R., Khodarahmi, R., Ramazzotti, M., Dobson, C. M., Cecchi, C., and Chiti, F. (2014) Toxicity of protein oligomers is rationalized by a function combining size and surface hydrophobicity. *ACS Chem. Biol. 9*, 2309−2317.

(15) Vieira, M. N., Forny-Germano, L., Saraiva, L. M., Sebollela, A., Martinez, A. M., Houzel, J. C., De Felice, F. G., and Ferreira, S. T. (2007) Soluble oligomers from a non-disease related protein mimic Aβ-induced tau hyperphosphorylation and neurodegeneration. *J. Neurochem. 103*, 736−748.

(16) Stefani, M., and Dobson, C. M. (2003) Protein aggregation and aggregate toxicity: new insights into protein folding, misfolding diseases and biological evolution. *J. Mol. Med. 81*, 678−699.

(17) Bucciantini, M., Giannoni, E., Chiti, F., Baroni, F., Formigli, L., Zurdo, J., Taddei, N., Ramponi, G., Dobson, C. M., and Stefani, M. (2002) Inherent toxicity of aggregates implies a common mechanism for protein misfolding diseases. *Nature 416*, 507−511.

(18) Nag, S., Sarkar, B., Chandrakesan, M., Abhyanakar, R., Bhowmik, D., Kombrabail, M., Dandekar, S., Lerner, E., Haas, E., and Maiti, S. (2013) A folding transition underlies the emergence of membrane affinity in amyloid-β. *Phys. Chem. Chem. Phys. 15*, 19129−19133.

(19) Jonsson, T., Atwal, J. K., Steinberg, S., Snaedal, J., Jonsson, P. V., Bjornsson, S., Stefansson, H., Sulem, P., Gudbjartsson, D., Maloney, J., Hoyte, K., Gustafson, A., Liu, Y., Lu, Y., Bhangale, T., Graham, R. R., Huttenlocher, J., Bjornsdottir, G., Andreassen, O. A., Jonsson, E. G., Palotie, A., Behrens, T. W., Magnusson, O. T., Kong, A., Thorsteinsdottir, U., Watts, R. J., and Stefansson, K. (2012) A mutation in APP protects against Alzheimer's disease and age-related cognitive decline. *Nature 488*, 96−99.

(20) Maloney, J. A., Bainbridge, T., Gustafson, A., Zhang, S., Kyauk, R., Steiner, P., van der Brug, M., Liu, Y., Ernst, J. A., Watts, R. J., and Atwal, J. K. (2014) Molecular mechanisms of Alzheimer disease protection by the A673T allele of amyloid precursor protein. *J. Biol. Chem. 289*, 30990−31000.

(21) Di Fede, G., Catania, M., Morbin, M., Giaccone, G., Moro, M. L., Ghidoni, R., Colombo, L., Messa, M., Cagnotto, A., Romeo, M., Stravalaci, M., Diomede, L., Gobbi, M., Salmona, M., and Tagliavini, F. (2012) Good gene, bad gene: new APP variant may be both. *Prog. Neurobiol. 99*, 281−292.

(22) Di Fede, G., Catania, M., Morbin, M., Rossi, G., Suardi, S., Mazzoleni, G., Merlin, M., Giovagnoli, A. R., Prioni, S., Erbetta, A., Falcone, C., Gobbi, M., Colombo, L., Bastone, A., Beeg, M., Manzoni, C., Francescucci, B., Spagnoli, A., Cantu, L., Del Favero, E., Levy, E., Salmona, M., and Tagliavini, F. (2009) A recessive mutation in the

DOI: 10.1021/acschemneuro.5b00074
ACS Chem. Neurosci. 2015, 6, 1290−1295

APP gene with dominant-negative effect on amyloidogenesis. *Science 323*, 1473−1477.
(23) Giaccone, G., Morbin, M., Moda, F., Botta, M., Mazzoleni, G., Uggetti, A., Catania, M., Moro, M. L., Redaelli, V., Spagnoli, A., Rossi, R. S., Salmona, M., Di Fede, G., and Tagliavini, F. (2010) Neuropathology of the recessive A673V APP mutation: Alzheimer disease with distinctive features. *Acta Neuropathol. 120*, 803−812.
(24) Paravastu, A. K., Leapman, R. D., Yau, W. M., and Tycko, R. (2008) Molecular structural basis for polymorphism in Alzheimer's β-amyloid fibrils. *Proc. Natl. Acad. Sci. U. S. A. 105*, 18349−18354.
(25) Chandrakesan, M., Sarkar, B., Mithu, V. S., Abhyankar, R., Bhowmik, D., Nag, S., Sahoo, B., Shah, R., Gurav, S., Banerjee, R., Dandekar, S., Jose, J. C., Sengupta, N., Madhu, P. K., and Maiti, S. (2013) The basic structural motif and major biophysical properties of amyloid-β are encoded in the fragment 18−35. *Chem. Phys. 422*, 80−87.
(26) Scheidt, H. A., Morgado, I., Rothemund, S., Huster, D., and Fandrich, M. (2011) Solid-state NMR spectroscopic investigation of Aβ protofibrils: implication of a β-sheet remodeling upon maturation into terminal amyloid fibrils. *Angew. Chem., Int. Ed. Engl. 50*, 2837−2840.
(27) Ono, K., Condron, M. M., and Teplow, D. B. (2009) Structure-neurotoxicity relationships of amyloid β-protein oligomers. *Proc. Natl. Acad. Sci. U. S. A. 106*, 14745−14750.
(28) Bleiholder, C., Dupuis, N. F., Wyttenbach, T., and Bowers, M. T. (2011) Ion mobility-mass spectrometry reveals a conformational conversion from random assembly to β-sheet in amyloid fibril formation. *Nat. Chem. 3*, 172−177.
(29) Pan, J., Han, J., Borchers, C. H., and Konermann, L. (2011) Conformer-specific hydrogen exchange analysis of Aβ(1−42) oligomers by top-down electron capture dissociation mass spectrometry. *Anal. Chem. 83*, 5386−5393.
(30) Barrow, C. J., and Zagorski, M. G. (1991) Solution structures of β peptide and its constituent fragments: relation to amyloid deposition. *Science 253*, 179−182.
(31) Gu, L., Ngo, S., and Guo, Z. (2012) Solid-support electron paramagnetic resonance (EPR) studies of Aβ40 monomers reveal a structured state with three ordered segments. *J. Biol. Chem. 287*, 9081−9089.
(32) Baumketner, A., Bernstein, S. L., Wyttenbach, T., Bitan, G., Teplow, D. B., Bowers, M. T., and Shea, J. E. (2006) Amyloid β-protein monomer structure: a computational and experimental study. *Protein Sci. 15*, 420−428.
(33) Sarkar, B., Das, A. K., and Maiti, S. (2013) Thermodynamically stable amyloid-β monomers have much lower membrane affinity than the small oligomers. *Front. Physiol. 4*, 84 DOI: 10.3389/fphys.2013.00084.
(34) Narayan, P., Ganzinger, K. A., McColl, J., Weimann, L., Meehan, S., Qamar, S., Carver, J. A., Wilson, M. R., St George-Hyslop, P., Dobson, C. M., and Klenerman, D. (2013) Single molecule characterization of the interactions between amyloid-β peptides and the membranes of hippocampal cells. *J. Am. Chem. Soc. 135*, 1491−1498.
(35) Bhowmik, D., Das, A. K., and Maiti, S. (2015) Rapid, cell-free assay for membrane-active forms of amyloid-β. *Langmuir 31*, 4049−4053.
(36) Adler, J., Scheidt, H. A., Kruger, M., Thomas, L., and Huster, D. (2014) Local interactions influence the fibrillation kinetics, structure and dynamics of Aβ(1−40) but leave the general fibril structure unchanged. *Phys. Chem. Chem. Phys. 16*, 7461−7471.
(37) Nag, S., Sarkar, B., Bandyopadhyay, A., Sahoo, B., Sreenivasan, V. K., Kombrabail, M., Muralidharan, C., and Maiti, S. (2011) Nature of the amyloid-β monomer and the monomer-oligomer equilibrium. *J. Biol. Chem. 286*, 13827−13833.
(38) Garai, K., Sahoo, B., Sengupta, P., and Maiti, S. (2008) Quasihomogeneous nucleation of amyloid beta yields numerical bounds for the critical radius, the surface tension, and the free energy barrier for nucleus formation. *J. Chem. Phys. 128*, 045102.
(39) Sahoo, B., Nag, S., Sengupta, P., and Maiti, S. (2009) On the stability of the soluble amyloid aggregates. *Biophys. J. 97*, 1454−1460.
(40) Sengupta, P., Balaji, J., and Maiti, S. (2002) Measuring diffusion in cell membranes by fluorescence correlation spectroscopy. *Methods 27*, 374−387.
(41) Sengupta, P., Garai, K., Sahoo, B., Shi, Y., Callaway, D. J., and Maiti, S. (2003) The amyloid β peptide ($A\beta_{1-40}$) is thermodynamically soluble at physiological concentrations. *Biochemistry 42*, 10506−10513.
(42) Tjernberg, L. O., Pramanik, A., Bjorling, S., Thyberg, P., Thyberg, J., Nordstedt, C., Berndt, K. D., Terenius, L., and Rigler, R. (1999) Amyloid β-peptide polymerization studied using fluorescence correlation spectroscopy. *Chem. Biol. 6*, 53−62.
(43) Garai, K., Sureka, R., and Maiti, S. (2007) Detecting amyloid-β aggregation with fiber-based fluorescence correlation spectroscopy. *Biophys. J. 92*, L55−L57.
(44) Sahoo, B., Balaji, J., Nag, S., Kaushalya, S. K., and Maiti, S. (2008) Protein aggregation probed by two-photon fluorescence correlation spectroscopy of native tryptophan. *J. Chem. Phys. 129*, 075103.
(45) Culbertson, C. T., Jacobson, S. C., and Michael Ramsey, J. (2002) Diffusion coefficient measurements in microfluidic devices. *Talanta 56*, 365−373.
(46) Sengupta, P., Garai, K., Balaji, J., Periasamy, N., and Maiti, S. (2003) Measuring size distribution in highly heterogeneous systems with fluorescence correlation spectroscopy. *Biophys. J. 84*, 1977−1984.
(47) Bhowmik, D., Maclaughlin, C. M., Chandrakesan, M., Ramesh, P., Venkatramani, R., Walker, G. C., and Maiti, S. (2014) pH changes the aggregation propensity of amyloid-β without altering the monomer conformation. *Phys. Chem. Chem. Phys. 16*, 885−889.
(48) Nelson, R., Sawaya, M. R., Balbirnie, M., Madsen, A. O., Riekel, C., Grothe, R., and Eisenberg, D. (2005) Structure of the cross-β spine of amyloid-like fibrils. *Nature 435*, 773−778.

DOI: 10.1021/acschemneuro.5b00074
ACS Chem. Neurosci. 2015, 6, 1290−1295